Lab on a Chip

Microfluidics in vascular biology research: a critical review for engineers, biologists, and clinicians

Journal:	*Lab on a Chip*
Manuscript ID	LC-CRV-04-2022-000352.R1
Article Type:	Critical Review
Date Submitted by the Author:	05-Jul-2022
Complete List of Authors:	Simitian, Grigor; University of Wisconsin-Madison, Biomedical Engineering Virumbrales-Munoz, Maria; University of Wisconsin-Madison, Biomedical Engineering Sanchez-de-Diego, Cristina; University of Wisconsin-Madison, Biomedical Engineering Beebe, David; University of Wisconsin-Madison, Biomedical Engineering Kosoff, David; University of Wisconsin-Madison,

Microfluidics in vascular biology research: a critical review for engineers, biologists, and clinicians.

Grigor Simitian [a,b,*], María Virumbrales-Muñoz [b,c,d,e*], Cristina Sánchez de Diego [b,d,e*], David J. Beebe[b,d,e] and David Kosoff[a, b]

Affiliations:

[a]Department of Medicine, University of Wisconsin-Madison, Madison, WI 53705

[b]Carbone Cancer Center, University of Wisconsin-Madison, Madison, WI 53705

[c]Department of Cell and Regenerative Biology, University of Wisconsin School of Medicine and Public Health, Madison, WI 53705, USA

[d]Department of Biomedical Engineering, University of Wisconsin-Madison, Madison WI

[e]Department of Pathology and laboratory Medicine, University of Wisconsin-Madison, Madison, WI 53705, USA

*Authors contributed equally to this manuscript.

Corresponding Author Email: dkosoff1@medicine.wisc.edu

Keywords: Angiogenesis, in vitro models, microfluidics, microphysiological systems, anti-angiogenics, vasculogenesis

Abstract

Neovascularization, the formation of new blood vessels, has received much research attention due to its implications in physiological processes and diseases. Most studies using traditional *in vitro* and *in vivo* platforms find challenges in recapitulating key cellular and mechanical cues of the neovascularization processes. Microfluidic *in vitro* models have been presented as an alternative to these limitations due to their capacity to leverage microscale physics to control cell organization and integrate biochemical and mechanical cues, such as shear stress, cell-cell interactions, or nutrient gradients, making them an ideal option for recapitulating organ physiology.

Much has been written about the use of microfluidics in vascular biology models from an engineering perspective. However, a review introducing the different models, components and progress for new potential adopters of these technologies was absent in the literature. Therefore, this paper aims to approach the use of microfluidic technologies in vascular biology from a perspective of biological hallmarks to be studied and written for a wide audience ranging from clinicians to engineers. Here we review applications of microfluidics in vascular biology research, starting with design considerations and fabrication techniques. After that, we review the state of the art in recapitulating angiogenesis and vasculogenesis, according to the hallmarks recapitulated and complexity of the models. Finally, we discuss emerging research areas in neovascularization, such as drug discovery, and potential future directions.

Introduction

The formation of new blood vessels, known as neovascularization, includes the physiological processes of angiogenesis and vasculogenesis, which have incredibly diverse human biology roles. The vasculogenesis process typically refers to the generation of novel blood vessels from scratch, especially during embryonic development, whereas angiogenesis is the development of new blood vessels from pre-existing ones. Under healthy conditions, the roles of these physiological processes are primarily supportive. For example, during development, angiogenesis can augment oxygen and nutrient delivery to developing organs, and following tissue injury, angiogenesis can repair damaged vascular networks and support tissue regeneration[1]. However, in the onset of diseases such as diabetes, asthma, cardiovascular disease, and cancer, angiogenesis can also play integral roles in tissue destruction and can be a vital factor in the morbidity and mortality of these conditions[2,3]. The incredible diversity of these roles and their importance in both normal biology and disease pathology have made angiogenesis an area of intense scientific research. The focus of this research is equally diverse, with topics that range from understanding the biology of angiogenesis to the development of therapies that target the pathways that drive the angiogenic process[4,5]. In this review, we focus most of our descriptions in angiogenesis, since its therapeutic possibilities are more explored in the literature, although we have dedicated a specific section to vasculogenesis, and have included novel vasculogenesis models in our sections, when appropriate.

Angiogenesis occurs as an orderly cascade of molecular events (Figure 1). In normal tissues, this cascade is tightly regulated by a balance of growth factors and angiogenic inhibitors. While angiogenic inhibitors (e.g., angiostatin, miRNA) circulate through the blood or are anchored in the ECM, angiogenic growth factors (e.g., vascular endothelial growth factor, fibroblast growth factor, and interleukin-8) are released by oxygen-deprived tissues or in response to hypoxia.

Released angiogenic factors activate endothelial cells in mature capillaries to initiate the angiogenic cascade. Following activation, endothelial cells secrete proteases (e.g., MMPs and heparinase) that degrade adjacent basement membrane and extracellular matrix (ECM). This remodeling, in turn, releases additional anchored pro-angiogenic factors, which further activates endothelial cells and increases vessel permeability to substrate diffusion. Activated endothelial cells migrate outward from the capillary and proliferate to form new sprouts oriented toward the source of the stimulus. After that, endothelial cells organize into hollow tubes and create new basement membranes for vascular stability. Newly formed blood vessels also recruit mural cells, (e.g., smooth muscle cells and pericytes), to stabilize the vascular architecture into mature functioning vessels capable of supporting blood flow.

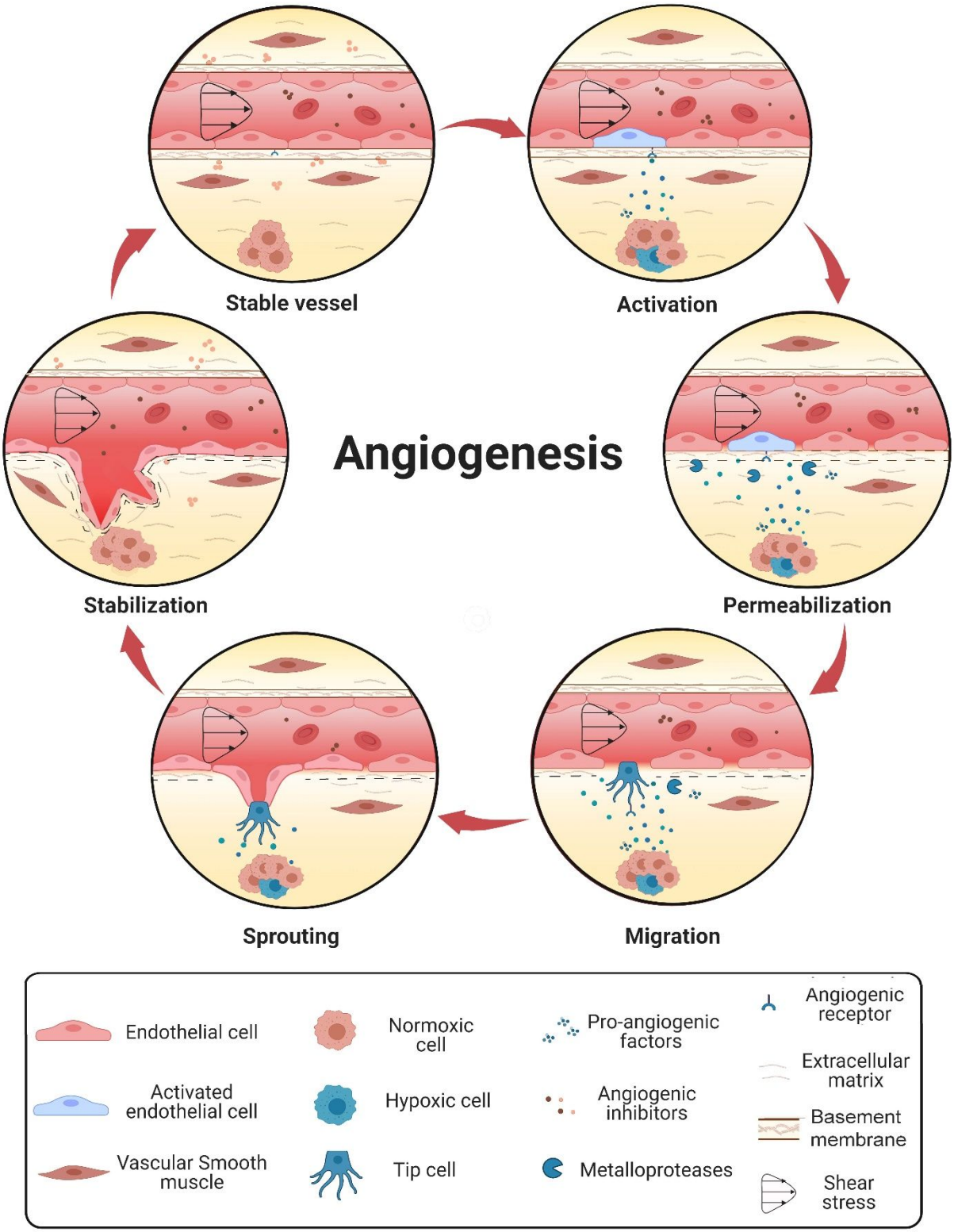

Figure 1. Angiogenesis occurs as an orderly cascade of molecular events: (1) activation of angiogenesis by angiogenic stimuli, (2) proteolytic enzyme production and subsequent degradation of the basement membrane and perivascular extracellular matrix (3) migration of endothelial cells and primary sprout formation (4) lumenation and formation of tube-like structures, and (5) novel basement membrane secretion and maturation into functional vessels capable of supporting blood flow.

Research in angiogenesis has led to the development of an array of therapies that have improved patient outcomes[6]. There are several available angiogenesis-directed therapies in cancer alone that can reduce tumor burden, improve symptoms, and increase survival for patients with an array of tumor types[7]. However, despite these important advances, there continue to be significant gaps in our knowledge of the angiogenic process that limit continued progress in these fields. Therefore, further research is needed to improve our understanding of angiogenesis and identify new pathways for therapeutic targeting.

Most of the studies published in the field of vascular biology research employ mouse models and 2D cell cultures as the primary platforms to study the mechanisms of angiogenesis, such as cell migration (e.g., Teflon fence, Transwell or wound healing assays) or microvasculature assembly (i.e., tube formation assay on Matrigel). These techniques are currently considered the gold standard of *in vitro* angiogenesis assays since they are cost-effective, high-throughput, and user-friendly. However, 2D techniques struggle to recapitulate key cellular and mechanical cues in the angiogenic process, dramatically affecting cell phenotype (Figure 1) [8,9]. Therefore, there remains a pressing need to develop and standardize models capable of mimicking features of the *in vivo* tumor microenvironment (TME)(i.e., the niche in which a tumor develops), such as nutrient gradients, 3D cell migration, or ECM-cell interactions, without sacrificing throughput and discriminatory capacity.

Microfluidic devices (i.e., those handling volumes in the μl scale) offer a range of solutions to the challenges posed by conducting research using traditional 2D and 3D mediums. Microfluidic devices have been used to model blood vessels and angiogenesis for the last few decades due to their balance of the best features offered by traditional *in vitro* and *in vivo* models (i.e., simplicity, tractability, and cost-effectiveness) additional small-scale benefits [10].

Furthermore, microscale physics confer additional advantages to these models for recapitulating organ physiology (e.g., fine control over distances, mechanical cues, tissue organization, and geometries) [11]. The device's small size also reduces the quantity of expensive reagents (e.g., cytokines, drugs, scaffolding proteins) and precious biological samples (e.g., patient-derived or circulating tumor cells) required for each assay. These advantages over traditional *in vitro* models make microfluidic devices ideal platforms for angiogenesis focused research.

Most reviews discussing microfluidic modeling of angiogenesis focus only on a description of technologies and publish studies without previously establishing basic microfluidic principles necessary to understand the models and their limitations. Here we present a comprehensive and critical review that balances a biological and an engineering perspective, and summarizes recent progress in the field, including the numerous papers mimicking (brain and other) microvascular networks using microfluidic devices.

Design considerations for microfluidic modeling

Microfluidic devices can harness the unique properties of fluids at the submillimeter scale. The highly predictable microscale physics (e.g., capillarity and laminar flow) dominate over classical macroscale physics (e.g., gravity), resulting in a great degree of control in the design and operation of the devices for the user.

Device fabrication

There are a limited number of fabrication techniques capable of fabricating microfluidic devices since few strategies have enough resolution to create these small structures. The most commonly used are soft lithography, micromolding, micromachining or milling, and, more

recently, 3D printing [12]. We will focus on the first two techniques, which are some of the most commonly used approaches to fabrication.

Soft lithography is based on using a photoresist and selective UV-curing (i.e., photolithography) to produce a detailed master mold, which is then used to shape a thermally cured polymer (i.e., soft lithography) (Figure 2A). The shaped polymer is typically bonded to glass to create a fully enclosed device [13]. This three-step technique is highly popular and presents many advantages: low price, ease of prototyping, and higher versatility [10]. The most commonly used materials for this technique are the photoresist SU-8 and the polymer polydimethylsiloxane (PDMS), with the latter being responsible for most advantages and limitations of the technique [14]. PDMS is reasonably priced, highly biocompatible once cured, optically transparent to light, and relatively inert[15]. However, many authors report PDMS interactions with hydrophobic molecules and high permeability to gases and fluids, presenting challenges in disease modeling and drug testing [16]. While many modifications have been proposed to PDMS over the years, this material remains one of the most popular options for fabricating microfluidic devices [17].

In contrast to soft lithography, the micromilling (also called CNC milling) fabrication process uses rotary cutters to remove bulk material and create microscale features[18]. Once the device is finished, it is typically bonded to plastic by high pressure, ultrasound, heat, or chemical solvents to create a fully enclosed device (Figure 2B). The wide diversity of cutting tools (size, materials, and shapes) makes the milling amenable to fabricating devices with different materials, shapes, and precision[19] Micromilling applications include the generation of molds[20] and the design of new prototypes and open microfluidic devices[21,22]. Despite the versatility and low fabrication times, the need for large equipment and highly specialized training have reduced the usage of micromilling compared to other methods for microfluidics[18].

Micromolding, on the other hand, is a set of techniques used to shape plastic polymers (e.g., cyclic olefin polymer or polystyrene) with the support of a mold (Figure 2C). Injection molding is one such technique, which involves the fabrication of a highly durable mold to shape the plastic polymers. This highly scalable technology is frequently used to manufacture everyday plastic objects, but the high durability required for the mold increases costs. Further, the technique presents limitations in size and the shape of the features that can be generated, since it is subject to the limitations of two engineering processes: the micromilling (also called micromachining) typically used to generate the mold; and the thermoplastic molding process, which results in the smoothing of certain angled interfaces (e.g., some squares become rounded after molding the thermoplastic). Therefore, micromolding is not chosen for small-scale and minute detail model development but rather for the commercial fabrication of robust and well-characterized devices [23]. Alternative strategies to solve some of these issues are being developed, especially in the generation of smaller and more accurate molds [24–26]. Since plastic polymers solve many of the challenges PDMS presents (e.g., molecule sequestration and high permeability), commercially available devices are on the rise. Currently, dozens of companies (e.g., Ibidi, MIMETAS) are flooding the market with micromolded, user-friendly products often developed from PDMS prototypes. [27]

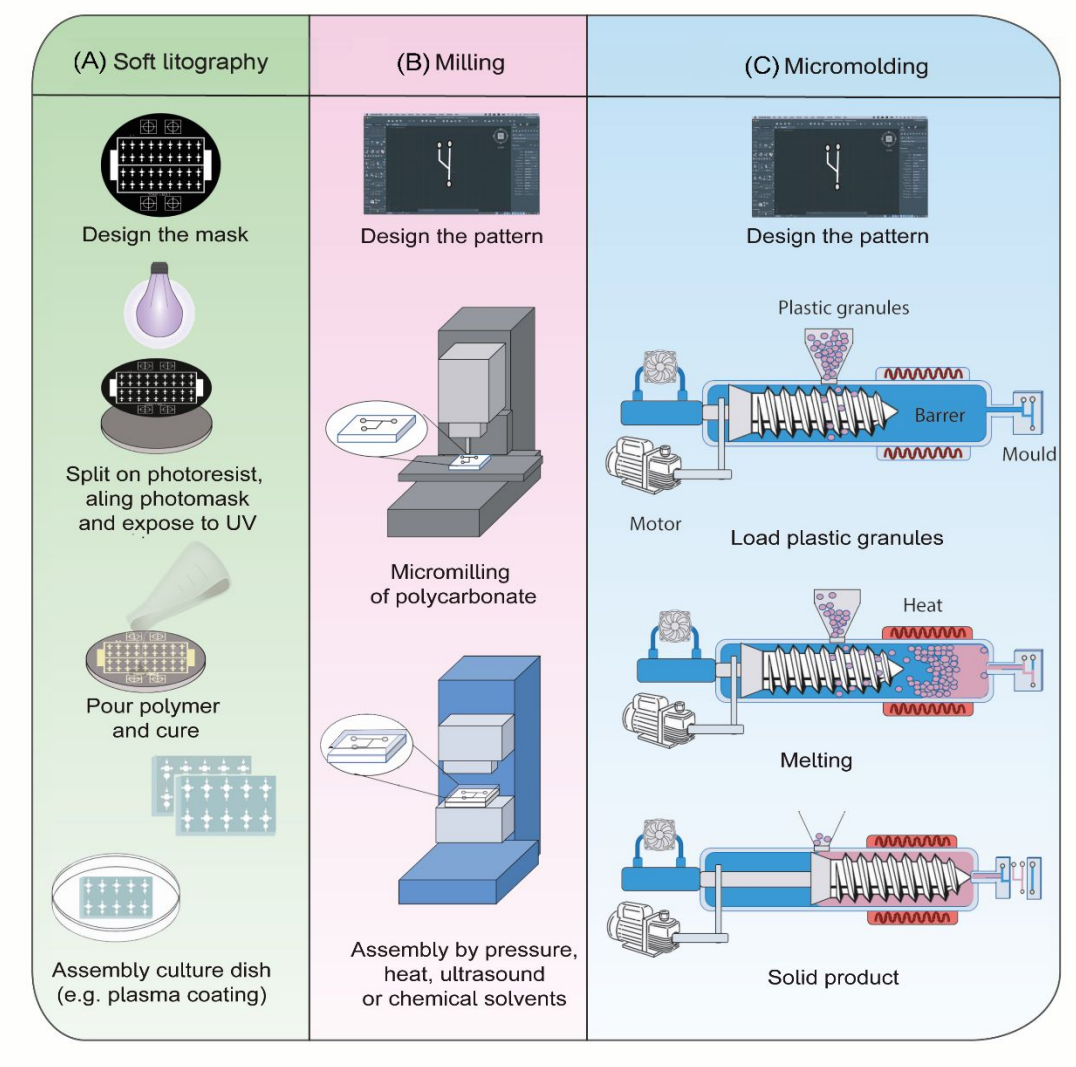

Figure 2. Schematic representation of the three main techniques described in this review to fabricate microfluidic devices. (A) Soft lithography: A mask is designed for each layer required to generate the desired SU-8 master mold. Then, subsequent layers of photoresist material are spun on a silicon wafer, and the UV mask is used to expose certain regions of the photoresist for UV light to polymerize. The non-exposed areas are later removed using a solvent. A mixture of PDMS and curling material is poured on the SU-8 master mold and let polymerize under heat. Polymerized devices are then extracted from the master mold, assembled, and bonded to a glass substrate to produce the final device. (B) Micromilling: A pattern is designed in AutoCAD. A sheet of material (e.g., plastic) is placed onto the machine support. The programmed micromill removes bulk material that can then be bonded to a substrate via high pressure, ultrasound, heat, or chemical solvents. (C) Micromolding (injection molding): A steel mold is designed with AutoCAD and machined. In the molding injector, plastic granules are melted and loaded into the mold. When the piece is cooled, it is ejected using pins that push it out of the mold, which can then be used again.

Porous interfaces: leveraging hydrogels and membranes in microfluidics

Although cells can be seeded directly on the surface of a device, microfluidic devices often contain hydrogels and membranes, which can also be used as substrates for cell attachment. Often, microfluidic designs will present adaptations to facilitate hydrogel injection and control its confinement. Hydrogels of synthetic or natural origin provide cells with a 3D architecture and mechanical and biochemical cues, similar to those *in vivo*. While many natural ECM options have been reported (e.g., hyaluronic acid, Matrigel, alginate), collagen and fibrin remain some of the most popular due to their ubiquity in primary tissues, robustness, and ease of use [9]. However, synthetic PEG derivatives and silk scaffolds have also been used as cell substrates in microdevices [28].

Microdevices with several channels or chambers typically leverage two different techniques to co-culture different cell types: microfluidic valves or porous membranes[29]. Microfluidic valves, a popular approach in microfluidics, leverage surface tension and geometry changes to pin a hydrogel at an interface. When the hydrogel polymerizes, a hydrogel-media interface is created and can be used as a substrate for cell seeding, often allowing cells to migrate into the hydrogel or remodel its architecture and composition[30]. A different approach relies on synthetic membranes, usually coated with ECM proteins, to enhance cell adhesion and separate the different compartments. Membranes vary according to their constituting material (e.g., polyesters, polycarbonates, PDMS), which in turn can influence their mechanical properties (e.g., flexibility) and pore size. Pore size (typically 5 - 0.1 μm) remains important for cell-based assays as membranes are often meant to retain most cells seeded on top of them while also allowing for the diffusion of molecules [31]. Conversely to the hydrogel pining approach, ECM remodeling studies are not often possible using membranes alone. Hybrid strategies of using a membrane for hydrogel pinning have also been reported [32,33].

Cell sources for microfluidic modeling of vasculature

Vessels range in size and complexity (e.g., arteries, capillaries), and are different according to the tissue of origin. However, the cells composing, and stabilizing blood vessels can be sorted within a handful of categories: Endothelial cells (hematogenous or lymphatic), vascular smooth muscle cells, pericytes and fibroblasts Within these lineages, cells also vary according to the tissue of origin. Together, this amounts to a large variety of vascular cells that could be used within microfluidic models. However, availability of cells for modeling is limited to commercial sources, iPSC-derived cells and primary cells from mouse models or human tissue samples (see table 1). Cell availability continues to be a hurdle for microfluidic modeling, resulting in only a few cell types that are highly popular for microfluidic studies.

Single endothelial tubes (constructed as endothelial cells lining a single channel) have served, as a starting point for studying vascular biology as previously discussed, and the cells of choice have traditionally been human umbilical cord endothelial cells. The popularity of HUVECs is likely due to their ease of availability, since they are both commercially available and easy to extract from donated umbilical cords, and their culture conditions and biology are well-known. Microvascular endothelial cells are also a popular alternative, and more recently the field has turned to induced pluripotent stem cells and commercial organotypic sources (Table 1). Next, fibroblasts have been a popular addition to microfluidic vascular models. The high variability of fibroblasts and additional sources have been nicely reviewed elsewhere[34–36].

More recently, smooth muscle cells, and pericytes have started to be included in vascular biology models. Recently more companies have started to commercialize cells of these lineages, yet sources of smooth muscle cells and pericytes remain more limited. We expect that the availability of these cells will continue to increase and facilitate the generation of new organotypic vascular models.

Table 1: Summary of vascular cell types and fibroblasts used in the microfluidic studies reviewed in this article. N=no, Y=yes

Cell type	Name	Tissue of origin	Organism of origin	Description	Commercial availability	Refs
Endothelial cells	hASC-EC	adipose	human	human adipose stem cell derived endothelial	N	[37]
	hBTAECs	breast	human	human breast tumor associated endothelial	Y	[38]
	CF cell-derived EC	cord blood	human	colony forming cell-derived endothelial	N	[39–42]
	iPSC-EC	dermal (iPSC)	human	human iPSC derived endothelial	Y	[43]
	GENCs	kidney	unknown	glomerular endothelial	Y	[44]
	KMVEC	kidney	mouse	kidney microvascular endothelial	N	[45]
	TENC/NENC	kidney tumor/adjacent normal	human	human primary kidney patient derived/normal adjacent endothelial cells	N	[46,47]
	HLMVEC	lung	human	human lung microvascular	Y	[48,49]
	HMVEC	microvascular -	human	human microvascular endothelial	Y	[50–54]
	HUVEC	umbilical cord	human		Y	[40,50,51,54–79]
	hTERT hMVEC	-	human	hTERT immortalized microvascular endothelial	N	[8,80]
	HLEC	-	human	human lymphatic endothelial	Y	[81,82]
Pericytes	pericytes	brain	rat	primary rat brain pericytes	Y	[43]
	HPP	brain	human	human pericytes	Y	[57]
	hVP	-	human	human vascular pericytes	Y	[59]
Smooth muscle cells	hVSMC	-	human	human primary vascular smooth muscle	Y	[59]
Fibroblasts	NDF	Skin	human	normal dermal fibroblasts	Y	[51,59,83]
	BJ-5ta		human	immortalized human foreskin fibroblasts	Y	[38]
	NHLF	Lung	human	Normal human lung fibroblasts	Y	[39–43,56,57,60,76]
	HNF	Head and neck cancer	human	Head and neck patient-derived fibroblasts	N	[82]

Microfluidic Models in Vascular Biology Research

The wide range of fabrication techniques and design options available for microfluidic platforms have enabled the development of a highly diverse array of devices for vascular biology research. This section will review the main types of microfluidic devices that have been applied applied in the field of vasculogenesis and angiogenesis.

Model classification according to cell seeding substrate

The study of vascular biology requires building vascular interfaces [84]. Said interfaces have been created using the polymers constituting the devices, 2D membranes, or 3D porous scaffolding (e.g., collagen, PEG-DA). Since cell substrates condition the events of the angiogenic cascade that can be modeled, we classified the microfluidic modeling approaches for angiogenesis based on the nature of the substrate used (Figure 3):

1) Cells are seeded on the device material (2D only): The polymer constituting the device, sometimes including 2D membranes, is the substrate for cell seeding. This approach, sometimes (and hereafter) called 2D vascular interfaces, was most often used in early reports where cell confluency, alignment, and responses to shear stress were assessed. It also allows for higher throughput, and hence is chosen over other experimental layouts for prototyping more complex geometries or adding large scale mechanical stimuli. [48] These setups excel at providing maximum throughput. However, the membranes used to create these platforms hinder endothelial cell migration and invasion, thereby limiting the relevance of some typical readouts of angiogenesis (e.g., sprouting).

2) Cells are seeded on a scaffolding material (3D only) and not the device building material: In this layout, a natural or synthetic matrix is used as a substrate for cell seeding, and the devices are only used to contain the scaffolding. The most common approaches to seeding the cells within 3D porous scaffolding are sacrificial molding of structures within the matrix (hereafter called 3D scaffolding models or devices) [85,86] and self-assembled vessels (hereafter

called microvascular assembly models or MVA models), which are discussed in detail in the following section. Other approaches have also been reported, such as the "viscous finger patterning" technique [87] or 3D bioprinting. While shear stress studies are possible using these layouts, they are more challenging and remain less ubiquitous in the literature. Conversely, other readouts are uniquely enabled by these technologies due to their full 3D structure: cell migration, sprouting, ECM remodeling are all ideally performed in these platforms. Conversely, their throughput tends to be lower than 2D or 2D/3D approaches. Notably, this approach is becoming more popular in later years.

3) Cells can be seeded on a scaffolding material (3D) and on the device building material (2D): The (often pinning based) architecture of these devices can be leveraged to pattern cells on a combination of polymer and 3D scaffolding (i.e., 2D/3D). Notably, some of these devices are the same as those used for 3D only (e.g., MVA models), but the interfaces of the material are used for cell seeding as well. The use of device materials has implications on cell morphology and physiology, due to the stiffer nature of devices and 2D organization of cells. A square cross-section vessel model is produced by using both hydrogel interfaces (produced by microfluidic valve or membrane pinning) and device walls. Several variations of this design have been reported with 3 or 5 microchannels, typically pinning 1-3 hydrogels through microfluidic posts [51]. A similar layout results from perfusing a 2D vascular interface device with a hydrogel. Finally, other devices have used pinning principles with a different design, such as the unique Stacks design, a modular design that allows assembly and disassembly of different hydrogel layers[88]. These 2D/3D setups present a balance in throughput as compared to 3D or 2D systems and benefit from the mechanical stability of using building materials as part of their seeding substrate. Therefore, they have shown the highest compatibility with angiogenesis-related readouts (e.g., shear stress, mechanical forces, permeability, sprouting). Conversely, there has been discussions in the literature indicating that

blood vessel models in these setups are not fully tubular nor fully established on a substrate of physiological stiffness, and therefore their functionality may be affected[89].

Certain readouts are equally enabled by all three approaches, such as immune cell recruitment and drug testing (Figure 3), since those applications are not especially affected by model constraints.

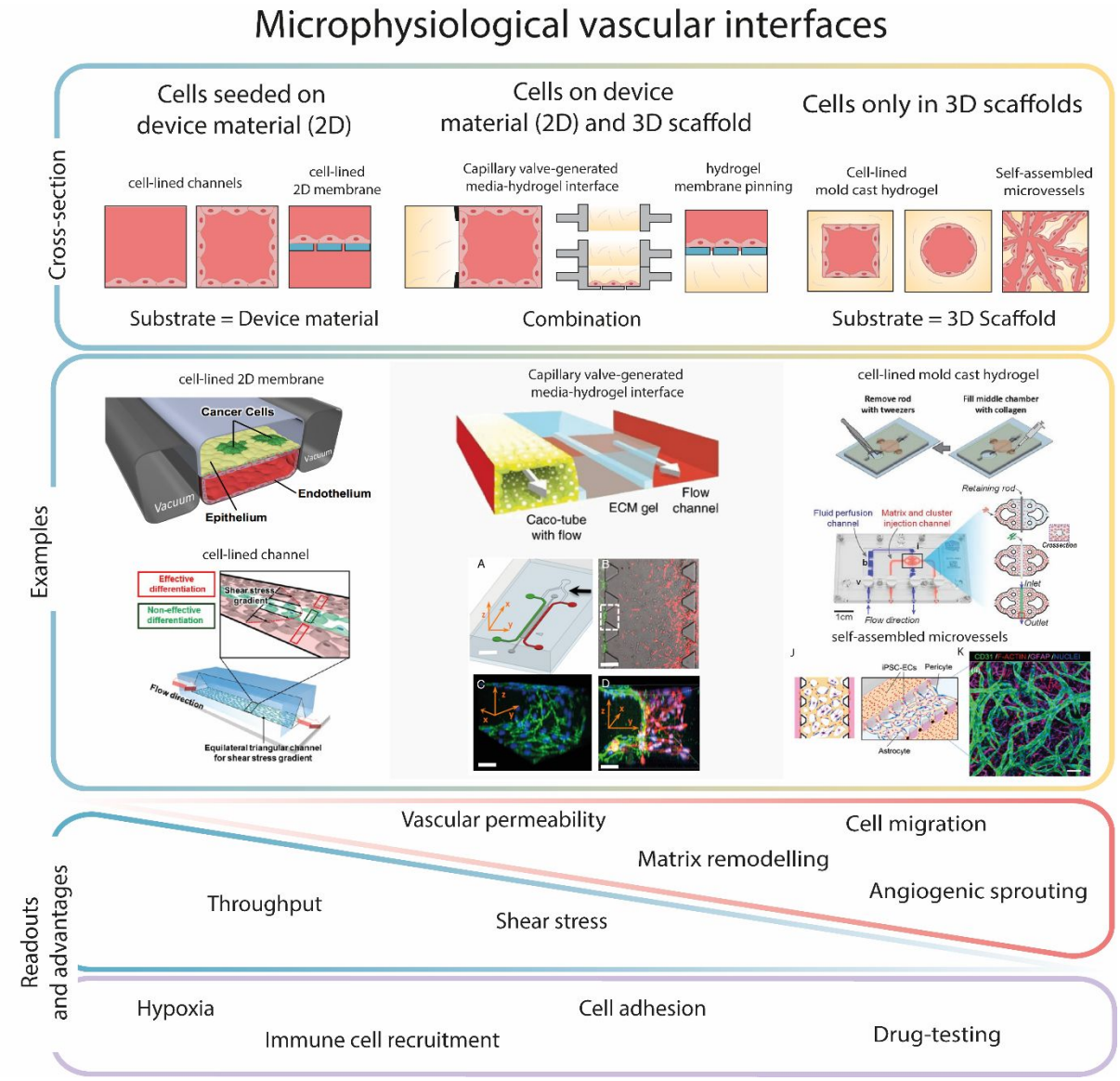

Figure 3: Classification of microphysiological models vascular interfaces used for angiogenesis research according to the substrate supporting the endothelial cells. In these models, cells can be supported on the device material (2D), a 3D ECM-like scaffold (of natural or synthetic origin) (3D), or both 2D and 3D (2D/3D). Different layout configurations are shown, with device walls depicted as bold black lines, ECM-like scaffolds in yellow, membranes in blue, culture media in red. Literature examples and advantages of each model are shown below[37,43,49,51,55,90,91]. The triangles symbolize the

applicability of those readouts to each configuration (apex = lower applicability), whereas the rectangle indicates that readouts are possible across the different configurations. Figures reproduced with permission.

Microfluidic models for Microvascular Assembly

Although most research to date has focused on angiogenesis as the main mechanism behind new vessel development, there is another important mechanism that has recently come into the spotlight in microfluidic models[92]. Specifically, vasculogenesis is an important biological process defined as the differentiation of precursor cells (e.g., angioblasts) into endothelial cells and the *de novo* formation of a primitive vascular network, whereas angiogenesis is defined as the growth of new capillaries from pre-existing blood vessels[93]. Vasculogenesis consists of three major steps: induction of vascular cell precursors like angioblasts (in a fibroblast growth factor (FGF)-dependent mechanism), assembly of primordial vessels (through vascular endothelial growth factor/vascular endothelial growth factor receptor signalling, VEGF/VEGFR) and transition from vasculogenesis to angiogenesis[94].

Microfluidic microvascular assembly (MVA) models were first reported in 2013 simultaneously by two independent laboratories [95], and leveraged designs with a central microchamber and flanking channels (Figure 3). In these models, the tubular network or MVA can be accessed via the flanking channels to add additional cell types, drugs, or antibodies for staining (Figure 3) [56]. Resulting blood vessel models present a smaller diameter that more closely resembles that of capillaries, and therefore their flow and transport rates of nutrients and oxygen to tissues are closer to those seen *in vivo*. Initial studies evaluated embedded culture of Human Umbilical Cord Endothelial Cells (HUVEC) and human lung fibroblasts in a fibrin and collagen 3D matrix in the central microchamber. Upon applying a fluid flow, HUVEC cells reorganized and self-assembled into a tubular network within 4-5 days, demonstrating that this model can be used to recapitulate tubular structures. Subsequent studies using alternative

endothelial cell models (e.g., iPSC-ECs) and additional cell types (e.g., pericytes) have also been successful in these models [43,57,58,96].

Several research groups have leveraged the MVA model to study vascular processes. Notably, to model anastomosis, *Wang et al*. created vessels on the flanking channels of the microvascular bed model and applied transendothelial flows and VEGF gradients to induce a vascular system model integrating an artery, a capillary network, and a vein [39]. The three vascular types were connected via two anastomosis-like junctions, as demonstrated by the barrier function exhibited by the conduit model. *DiVito et al.* created an MVA model via hydrodynamic focusing, a technique that leverages relative pressures of two or more fluids within a channel to align particles or cells in a specific area and simulated angiogenesis tubulogenesis, and anastomosis [59]. Later, other authors repurposed this model to mimic tumor angiogenesis [40,60] and metastasis [61], with an emphasis on anti-angiogenesis drug testing [41,62], which is discussed in the dedicated section of this review.

Microfluidic applications in vascular biology research

One of the key advantages of microfluidics over traditional cell culture platforms is the high user control and customizability, which allows the user to incorporate many different environmental factors that play a role in the biological process of interest, including a variety of cell types and biophysical or biochemical cues[11]. Further, another advantage of microfluidics is the capability to evaluate functional readouts, which is typically defined as those that directly evaluate the physical response of cells to specific microenvironmental stimuli or treatments (e.g., cell migration, cell-cell junctions)[97].

This section will review the various hallmarks of vasculogenesis for which microfluidic devices have been designed and discuss the roles of select devices in angiogenesis and

vasculogenesis including the effect of biophysical and biochemical cues and functional readouts uniquely enabled by these technologies (Figure 4).

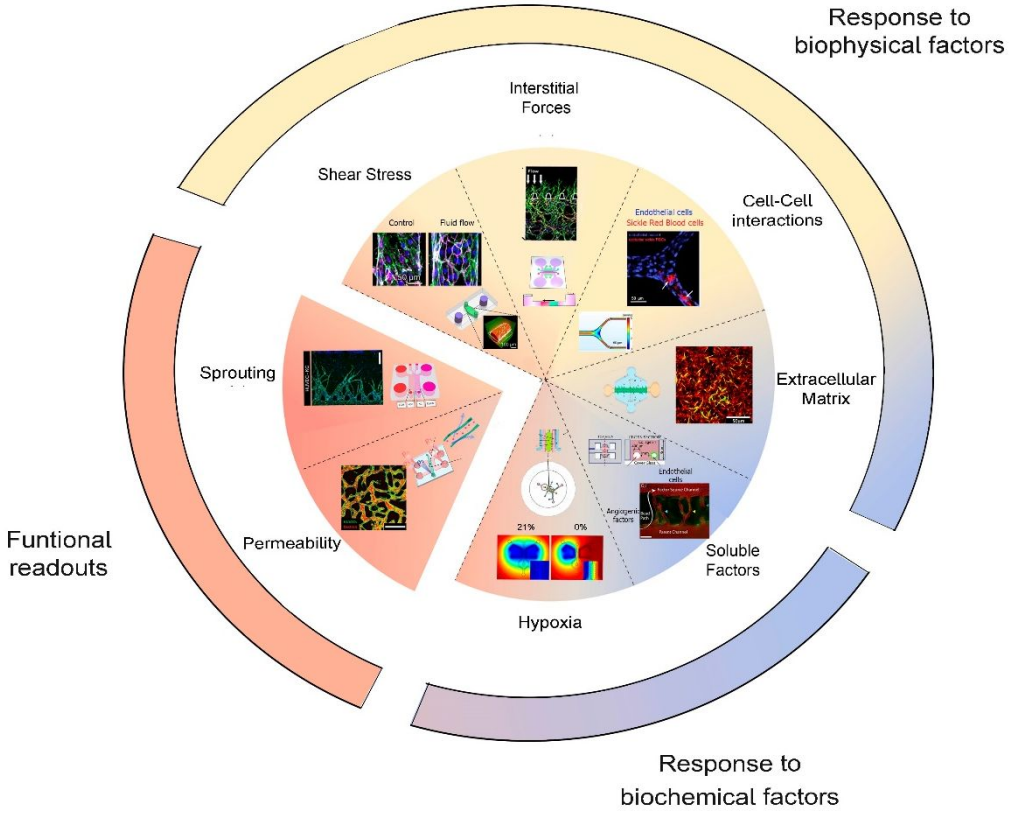

Figure 4: Summary of the applications (larger portion of graph) and main functional readouts (extruded section) in microphysiological models used to investigate contributing factors to neovascularization. Main biophysical factors studied in microfluidics include the response to Shear Stress [98], Interstitial Forces [75] , Cell-Cell interactions[99], Extracellular matrix[84]. The principal biochemical factors studied are Soluble Factors [85] and Hypoxia [100]. The main functional evaluated in microfluidic models are vessel permeability [56] and angiogenic sprouting [101]. Figures reproduced with permissions.

Biophysical factors in vascular biology

Mechanical forces in blood vessels are tightly controlled due to their crucial role in maintaining vessel homeostasis. These forces are dependent on the flow pattern of fluid within the vessels, which in most of the circulatory system is laminar. Laminar flow is characterized by a parallel orientation to the vessel, with a series of molecular layers slipping past each other with increasing velocity towards the center of the vessel (a detailed description of the physics

involved in fluid flow patterns can be found in [102]. This flow pattern results in two types of fluid-exerted forces: intravascular and transvascular.

Intravascular forces are those exerted within the vessel due to fluid flow. The most studied intravascular forces are shear stress, which is the stress exerted on the endothelium due to tangential blood flow. Endothelial shear stress depends on the flow rate, the blood's viscosity, and the tube's geometry. In general, mean shear stress is higher in small arterioles (60- 80 dynes/cm^2) [103] and lower in large veins (<1 dyne/cm^2) [104]. Blood behaves as non- Newtonian fluid in small capillaries and is, therefore, less predictable than other fluids (e.g., water). Shear stress induces several biological responses in endothelial cells mediated by the mechanosensing proteins integrins, including cytoskeletal reorganization, regulation of differentiation, proliferation, migration, and angiogenic sprouting. Conversely, dysregulation of shear stress is observed in pathologies, such as atherosclerosis [105].

Transvascular forces, mainly interstitial pressure, are those exerted outward of the vessel by the fluid and primarily depend on the contained fluid volume. Fluid volume results from the equilibrium of two phenomena: hydrostatic pressure of blood, forcing fluid out of the capillaries, and the oncotic pressure driving fluid from the interstitial space back into the capillaries and lymphatics. [106]

The following section reviews some of the most important microfluidic devices reported to study fluidic forces and their effects on angiogenesis.

Shear stress and interstitial forces in microfluidic vascular models

Microfluidic devices have inherent advantages for studying the effects of fluid flow on cell culture systems: a scale where laminar flow is dominant and highly customizable designs to recapitulate the vessel and cues of interest. Furthermore, these systems provide an easy interface with precision flow pumps, such as syringe or peristaltic, which deliver constant or

pulsatile flow, respectively. The height of the microchannel and fluid flow pressure enabled by the pump determines the applied shear stress, thereby providing fine control over the fluid forces in these systems.

Most studies have evaluated the effects of shear stress on angiogenic hallmarks (Figure 1) other than the traditional angiogenic migration and sprouting. Early studies of shear stress in microfluidic cell cultures seeded a single cell type monolayer on a 2D vascular interface on PDMS, often coated with ECM proteins to enhance cell adhesion [107]. High-throughput versions with several channels running in parallel [63] have been reported, and commercial versions of this device with different channel heights are available for modeling different shear stress ranges (e.g., IBIDI's μ-Slide I Luer). 2D vascular interfaces have been used to investigate the effects of shear stress on multiple cell functions, such as cytoskeletal organization, immune cell recruitment, or drug uptake. *Buchanan et al.* were the first to modify this design to generate a spatiotemporal mapping of flow fields [44,80]. Other modifications in the geometry of the channels (e.g., diamond-shaped channels, corners, pillars) can be used to accommodate high and low-stress zones within the same chamber [63]. An example of these modifications was reported by *Westein et al.* to model stenotic lesions [64] *in vitro*. Other authors have leveraged 2D membrane devices to combine the effects of stress with paracellular transport of small molecules [65], cell-cell interactions, or cell migration across the membrane have been described [66]. Using these devices, *Shirure et al*. demonstrated that angiogenesis is directionally opposite to interstitial flow in stiff matrices at physiological interstitial flow (0.1–10 lm/s). [42]

2D/3D microfluidic models have been used to analyze the effects of interstitial flow together with shear stress, angiogenic gradients, and cell-cell interactions within the TME. To this end, they used a 3-channel platform and used each of the channels as follows: 1) endothelialized channel, 2) 3D matrix, often including additional cell types of interest 3) optional channel for lymphatic drainage. [52,68,108] These type devices have been helpful in the field of cancer research

to mimic native tumor vascular flow dynamics and investigate cancer-ECM-endothelial interactions. [38,53]

3D scaffolding microdevices have been less popular to study flow-induced shear stress. Yet, they offer an independent modulation of flow-induced shear in a 3D microenvironment. *Buchanan et al*. created a microchannel lined with endothelial cells and surrounded by a collagen matrix containing embedded tumor cells[109]. Using this platform, the authors investigated the role of shear stress on vascular barrier function and tumor-endothelial crosstalk. However, the tubular geometry of *Buchanan et al.* device did not allow transmural shear since the flow was tangential to the apical surface of the endothelial-lined microchannel. Using a combination of 3D and 2D microfluidic devices*, Galie et al*. found that both transmural and luminal flow are required to induce and sustain flow-induced sprouting [50]. Recently, 3D scaffolding devices have been leveraged to generate curved vessels with a controlled diameter (120-400 μm), curvature, and torsion. This system reproduced the changes in wall shear stress induced by curvatures and generated a stress gradient in 3D. The authors found that, under high shear stress, spiral vessels increase the proliferation rate of endothelial cells. However, no clear relationship between fluid-induced forces and angiogenic sprouting has been established yet in microfluidic platforms. [50,110]

Cell-cell interactions in microfluidic vascular models

Several types of cells (e.g., erythrocytes, platelets, and immune cells) circulate in the blood and contact the endothelium. Although erythrocytes are the most abundant cells in human blood, platelets and immune cells circulate preferentially at the periphery of the bloodstream due to their small mass and therefore have higher chances of interaction with the endothelium [111]. Thus, vascularized microfluidic models represent ideal models to investigate the effects of blood cells on angiogenesis.

Early studies used 2D vascular interfaces (or commercial analogs) perfused with whole blood or a specific blood cell type to analyze blood- endothelium interactions. For instance, these devices have been used to study alterations in endothelial glycocalyx and cellular adherence and therapeutic strategies for sickle cell disease or malaria [69,70,112]. However, the impact of these alterations in the angiogenic process remains unknown.

Although 2D microfluidic devices can be useful to analyze the molecular cues involved in Endothelium-Blood cell interactions, they lack the 3D structure needed to recapitulate important processes such as matrix invasion during angiogenic sprouting, leading to the development of 3D scaffolding devices to model angiogenesis. The earliest 3D scaffolding devices leveraged PDMS to create microvascular-sized fluidic channels lined with endothelial cell monolayers in their inner 3D surface. This system reproduced quantifiable velocity profiles of red blood cells and cellular mechanisms of adhesion and aggregation; therefore, it has become a suitable device for studying microvascular occlusion and thrombosis [72,113]. However, solid polymeric materials present challenges to recapitulate relevant tissue stiffness, leading to endothelial dysfunction and compromised barrier function. To address this issue, *Qiu et al*. used an agarose-gelatin interpenetrating polymer network (IPN), which confers a more physiological relevant stiffness (from hundreds of Pa to 50 kPa) and maintain barrier function for over one month under continuous laminar flow condition (Figure 3) [99]. The introduction of porous membranes enabled the communication of different microfluidic chambers. One example is the Vessel-Chip reported by *Barile et al*., where a human endothelial model is perfused with whole human blood at physiologically relevant shear to model thrombosis [114]. Another 2D/3D microfluidic model was used to recreate the effect of immune cells and factors on endothelial cell migration. This device connected two endothelialized side channels through one migration channel. Endothelial cells and immune cells are placed in one channel, while

VEGF and other cytokines were perfused in the other to investigate their effect on cell migration [115].

Notably, these studies provided only a first approach of evaluating the effects of blood-endothelial interactions in regulating neovascularization. Therefore, there is still opportunity to evaluate the effects of blood-endothelial interactions on other angiogenic hallmarks (Figure 1) including traditional angiogenic migration and sprouting.

Extracellular matrix in microfluidic vascular models

The extracellular matrix (ECM) is a network of proteins, including glycosaminoglycans, proteoglycans, and collagen, which vary across different tissue provide biochemical, biomechanical, and structural cues for the development of organs [116].

ECM composition and architecture are known to have important roles in the development of new vasculature and the stabilization of established networks [117]. While the role of ECM in angiogenesis remains understudied using microfluidic technologies, a few strategies have emerged for recapitulating the effects of native ECM in microfluidic devices. A first approach leveraged 2D microfluidic devices of PDMS or glass coated with a single or combination of purified ECM proteins (e.g., collagen, fibronectin, or laminin) to enhance cell adhesion [113]. However, PDMS has a higher stiffness than vascular ECMs (i.e., MPa instead of the physiological kPa range). To overcome this issue, three main approaches have been developed: (1) increasing the ratio of PDMS elastomer to curing agent[118] (2) coating 2D PDMS devices with acrylamide/bisacrylamide gels [119] (3) and embedding streptavidin-coated magnetic beads to modify the stiffness of the ECM upon the application of an external magnetic field [120]. Besides ECM stiffness, heterogeneity of pore diameter, number, and alignment results in differential effects on angiogenesis. To examine the relationship between pore size and migration, *Keys et al.* developed a PDMS microfluidic device containing a series of thin

channels (1-3 μm in width) that mimic constraints in cell migration with different physiological pore sizes. [121]

3D hydrogels have also been applied to create endothelialized tubes typically encapsulated in collagen. These devices mimic the multiscale organization of vascular ECM and have shown to be effective models for investigating solute diffusion rates between the lumen and the ECM, cell-ECM interactions, and ECM remodeling (Figure 4) [98,122]. Similar endothelialized tubes have been leveraged to develop tumor organoid-vessel co-cultures to study vascular recruitment and tumor intravasation [123]. Early devices used type I collagen and fibrin hydrogels to reproduce the ECM and showed that higher concentrations of polymers resulted in decreased sprouting. However, the specific molecular cues responsible for this effect (e.g., matrix stiffness, porosity, degradability, viscoelasticity, and ligand engagement) remained unidentified[124]. Later, synthetic hydrogels (e.g., functionalized polyethylene glycol, hyaluronic acid, alginate, and dextran) were introduced and compared with their natural homologs, revealing that matrix permeability was a critical regulator of angiogenesis [125–127]. To reproduce a more physiological ECM, 3D hydrogels can be functionalized with integrin- or protease-binding sequences in studies of cell binding capacity and matrix degradability in angiogenesis[128]. Other authors leveraged 3D PDMS devices with microchannels to generate diffusion gradients of pro-angiogenic factors (e.g., VEGF) across the ECM and analyze its effect on endothelial sprouting [129].

The ECM properties (stiffness, density, and microstructure) alter angiogenic behavior in microvessels, however, little experimental data are available and there is a gap in our knowledge about microvessel interaction with its matrix. We anticipate that recent advances in microfluidic devices, imaging and computational methods will enhance the control of ECM properties and enable further study of its implications on angiogenesis and vasculogenesis.

Biochemical factors in vascular biology

Biochemical factors contribute regulate the process blood vessel formation via spatial cues that direct vessel sprouting and maturation. Stimuli such as hypoxia or inflammation, provoke a localized release of cytokines and other soluble molecules, which effectively creates a gradient within the extracellular space. The establishment of this molecular gradient leads to the formation of a spatially controlled leading edge of cells, which induces localized angiogenesis and increased perfusion.

Soluble factors in microfluidic vascular models

At its core, blood is a connective tissue with vital roles in a variety of processes, including cellular nutrition, drug delivery, clot formation, immune and inflammatory response, and regulation of angiogenesis. These functions are tightly regulated through a complex communication between the blood, distant organs and the vascular endothelium mediated by adhesion mechanisms, fluid forces, and pro-angiogenic factors (e.g., VEGF, FGF). The alteration of this delicate balance results in pathological conditions affecting vascular systems and distant organs, including liver disease, cystic fibrosis, pulmonary arterial hypertension, and sickle cell disease.

Plasma is the acellular portion of blood, composed of an aqueous solution of small organic molecules, proteins, and salts. Plasma regulates angiogenesis through two main mechanisms: fluid forces and the presence of soluble proteins or factors. These soluble factors can be classified into 4 categories: angiogenic growth factors (e.g., VEGF, FGF, Ang-1), pro-inflammatory cytokines (e.g., TNF-alpha, IL-6), chemokines, and second messengers to angiogenic molecular pathways (e.g., S1P, cGAMP) [130]. While growth factors are the main drivers of angiogenesis, pro-inflammatory cytokines play a larger role in regulating vessel permeability. Finally, chemokines are responsible for recruiting immune cells, which, in turn,

secrete angiogenic growth factors [131]. Most of the microfluidic designs described in this review have been leveraged to investigate the role of soluble factors in angiogenesis, with a particular interest in the role of angiogenic growth factors.

2D/3D devices were first used to study sprouting angiogenesis in response to VEGF and Angiopoietin-1 gradients [68,73,132]. Recently, an innovative capillarity-based design capable of stacking several hydrogel disks and re-assembling them studied the effects of cell-secreted chemokines (i.e., CXCL10, CXCL11, and IL-10) on HUVEC cells seeded in a hydrogel interface [88]. Less often, 2D/3D devices have been used to investigate the effects of pro-inflammatory cytokine TNF-α on endothelial integrity and cell junctions [54]. These studies revealed an alteration in endothelial cell morphology, followed by an increase in endothelial barrier permeability, and pointed to a fibrosis mechanism. However, 3D scaffolding models have proved more popular for these studies. For example, tubular mold casting devices in collagen hydrogels have investigated the effects and mechanism of pro-angiogenic growth factors, such as VEGF and sphingosine-1-phosphate (Figure 4) [45,85], revealing increased angiogenic sprouting.

Finally, several MVA models have been recently reported to investigate the effects of angiogenic growth factors, such as VEGF [96] and PDGF-BB [74], either adding them exogenously or using specific inhibitors [57]. While most reports have investigated the role of angiogenic growth factors, few have studied the role of pro-inflammatory cytokines (Figure 4), [75] chemokines, and other important secondary messengers in angiogenesis. Of note, a recent report from *Campisi et al*. examined the role of tumor-secreted secondary messenger cGAMP in an MVA model. The authors noted how this molecule promoted an increase in oxidative stress in their model and activated the endothelial cells in the microvasculature model [76].

Hypoxia in microfluidic vascular models

All tissues in the human body rely on oxygen to support their metabolic requirements. Decreases in local oxygen tension in tissues (i.e., hypoxia) therefore results in the activation of an array of compensatory intra- and extracellular pathways to increase oxygen supply. Angiogenesis is a key component of this compensatory response, restoring oxygen through increased blood flow to hypoxic areas. Studies evaluating hypoxia *in vitro* have encountered important challenges with replicating relevant oxygen levels: while atmospheric oxygen tension is 20%, normoxia within tissues varies between 3% to 7.4%, and tumor oxygenation is further reduced at <2% [133]. Conventional methods of replicating tissue oxygenation *in vitro* use chemical preconditioning (e.g., $CoCl_2$ treatment) or incubators that modify oxygen tension by mixing in carbon dioxide or nitrogen gas, both of which present limitations. Chemical preconditioning often presents off-target effects, including cytotoxicity, and specialized incubators are expensive and cannot guarantee a loss of relevant oxygen tension as samples are manipulated for maintenance or imaging [134].

Microfluidic technologies can overcome many of these limitations, supporting both fine-tuning of oxygen tension and analysis of the effects of hypoxia in cell cultures. However, this remains an active field of research since PDMS is not ideally suited to study the impact of hypoxia due to its high oxygen diffusivity [135]. Therefore, constant control of oxygen tension is required to maintain a hypoxic environment within PDMS devices. Alternatively, oxygen-impervious materials (e.g., COP) [136] or PDMS modifications have been proposed to mitigate this issue [137].

Notably, there is very little literature evaluating the effects of varying oxygen concentrations in traditional angiogenic hallmarks, such as sprouting (Figure 1). Therefore, most of the approaches described here are first uses of microfluidic technologies in vascular biology studies. 2D interfaces on porous membranes and 2D/3D models have been used to study the effects of hypoxia. These designs used one of the channels to perfuse oxygen scavengers (i.e.,

molecules capturing oxygen, such as sodium sulfite) or gasses capable of displacing oxygen in culture (e.g., CO_2). In contrast, the other channel was used for cell culture [134]. This methodology allows for rapid equilibration times and supports the creation of oxygen gradients. An early example of this application was reported in 2012 (Figure 4) [100] and demonstrated that hypoxia enhanced breast cancer cell migration.

One of the few reports studying effects of hypoxia in the endothelium was recently reported by *Lam et al.* The authors used a 5-channel pinning device to create a 2D/3D model, where an endothelial layer was cultured in the central channel, flanked by two stromal chambers. One of the outermost channels was used to perfuse media containing sodium sulfite (thereby depleting oxygen), whereas the other was used to perfuse normally oxygenated media [138]. This setup established a left-to-right oxygen gradient and enabled spatiotemporal control of oxygen tension around a vessel network, including cycling around two oxygen values to simulate intermittent hypoxia described in some pathologies.

To simulate hypoxia within a more advanced vessel architecture, *Wu et al.* created 2D PDMS channels with shapes resembling normal and tumor-associated capillary beds. The authors used a dialysis membrane to separate the cell culture from a fluid flow of sodium sulfite-supplemented media. The dialysis membrane allowed the exchange only of oxygen scavengers. Different oxygen tensions were achieved by varying the media flow rate or scavenger flow rate, validating this platform to simulate tumor hypoxia and vascular anomalies.

A recent report from *Hsu et al*. developed a microfluidic device fabricated in 4-layers alternating PDMS and laser-etched acrylic and used it to generate an MVA model[139]. A combinatorial screening of hyaluronic acid concentrations in the hydrogel and different oxygen tensions evaluated their effects on the MVA density. Their experiments revealed that oxygen gradients promoted the proliferation and assembly of the endothelial cell networks within the

hydrogels, whereas the hyaluronic acid promoted networking but not proliferation. Furthermore, the combination of oxygen gradients and hyaluronic acid further promoted vascularization, reinforcing the importance of different biochemical cues and gradients in the angiogenic process.

Other authors have leveraged cell consumption to generate hypoxic gradients similar to those observed in tumor tissues as an alternative to oxygen scavengers. For example, we recently leveraged a 3D scaffolding setup with two tubular structures: one mimics a blood vessel, whereas the other had a densely packed mass of renal cell carcinoma cells. In this setup, we observed the generation of hypoxia, secretion of growth factors, and an increase in the angiogenic response of the nearby blood vessel model[140]. Overall, the effects of different levels of hypoxia in the different neovasculogenic mechanisms remain largely understudied and may be therapeutically targetable, therefore creating opportunities for future studies in this topic.

Functional readouts

Functional readouts are those that directly evaluate treatment response on live cells (e.g., cell migration, cell proliferation) and consider additional factors such as the tissue of origin, the tumor microenvironment, or the immune system. These readouts are capable of quantifying the performance or behavior of cells to directly evaluate response to an environmental stimulus or treatment and can help provide more robust indicators of biological effect, or in the case of drugs, predictors to identify the optimal treatment [141]. Two such readouts in vascular biology are vessel barrier function and permability; and angiogenic sprouting[97]. The following section reviews the use of microfluidic devices to the effect of blood and barrier function permeability in blood vessel formation and remodeling.

Barrier function and permeability

The structure of blood vessels, which comprises tightly joined endothelial cells and a basement membrane, creates a barrier that restricts the movement of water, solutes, proteins, and blood cells between the intravascular and interstitial compartments. The endothelial barrier contributes to the function and homeostasis of several organs (e.g., kidney, intestine, eye, brain). Therefore, diminished barrier function can lead to severe pathologies such as organ failure, sepsis, inflammatory, neurodegenerative diseases [142]. The evaluation of barrier function has been one of the most popular readouts in microfluidic models, including blood vessels. For example, 2D/3D microfluidic models have been helpful for reproducing biological barriers such as brain, intestinal, or lung epithelial barriers[143–147]. The most studied barrier functions include the blood-brain barrier (BBB), lymphatic system, kidney-barrier, and eye-barrier. In this review, we focused on the physiological systems where barrier function plays a role in angiogenesis, thereby excluding popular barrier function models, such as BBB, which have been reviewed elsewhere [143,148]

Other barrier studies have leveraged 3D microfluidic devices to analyze tumor-blood vessel crosstalk and drug response, either as organoids or disperse cells in a 3D collagen matrix. In particular, the study of drug transport and efficacy within TMEs has generated considerable research interest). Recent studies show that the presence of tumor cells and conventional chemotherapeutics increase vascular leakiness [77]. However, antiangiogenic drugs can rescue normal vessel permeability [47]. Microvascular endothelial barriers have also been modeled using 3D devices.

An example was reported by *Kim et al*., who used microneedles to create an array of microchannels embedded within the bulk of a collagen matrix. As well as enabling the transport of nutrients, chemical compounds, biomolecules, and cell suspensions, this device supported the application of flow-induced mechanical stimuli [149]. Recently, 3D microfluidic devices have

been applied to model blood vessel barriers in other organs, such as the blood-retinal barrier, crucial for maintaining adequate vision [150]. This unique model enabled 3D co-cultures of monolayers of human retinal pigment epithelium cells with human endothelial cells lining a microvessel[151]. In addition, microvessels demonstrated a well-defined geometry and physiological permeability, which increased in a dose-dependent manner with oxidative stress exposure, making this a useful model for the study of age-related macular degeneration.

Angiogenic sprouting and remodeling

Sprouting angiogenesis is the main process by which new blood vessels grow from existing ones. It occurs in several well-characterized stages and is controlled by the presence of angiogenic and antiangiogenic molecules. Moreover, vessel sprouting undergoes extensive remodeling during angiogenesis until they form a mature vasculature. This process includes steps of vascular pruning and regression of selected branches. Traditional *in vitro* cell cultures can be used to investigate endothelial cell migration and proliferation. However, they fall short of recapitulating the 3D environment of endothelial cells and integrating mechanical and chemical stimuli precisely. Therefore, microfluidic devices have been presented as a solution to overcome most of these challenges.

Due to the limitations of most 2D devices to assess 3D sprouting, 3D devices have been preferably selected. The first studies used collagen hydrogels within PDMS devices where endothelial cells were cultured in 3D parallel channels [68]. Using this methodology, the authors measured endothelial sprout length into the ECM [67]. To evaluate the effects of chemical cues and fluidic forces, gradients of angiogenic factors have been established in the systems [74,85], and fluidic forces have been applied (e.g., perfusion) [78]. Complex geometries enabled the generation of temporally or spatially defined pro-angiogenic factor gradients [129]. A combination of VEGF-165 phorbol 12-myristate 13-acetate (PMA) and sphingosine-1-phosphate (S1P) promoted sprouting while perfusion acts as an essential survival and vascular

stabilization factor. In addition, tumoral organoids, or other cell types have been embedded within the collagen matrix, revealing a pro-angiogenic effect measured as an increase in angiogenic sprouting [55].

While these systems are highly informative, the parallel endothelial channels did not fully reproduce the physiological organization of vasculature. The use of 3D capillary beds set in multiple planes has been proposed to overcome this drawback and reproduced the "tree-like" capillary structure shown *in vivo* [152]. Another limitation of most microfluidic devices was the rectangular shape of their chamber, which did not reproduce the physiological circular tube-like structure [29,89]. Consequently, the traditional chambers were substituted by a series of interconnected open-top microwells filled with collagen. The authors found that the distribution of sprouts in this model was more regular and generated more tube-like structures[153].

Therapies targeting angiogenesis

Upregulation of angiogenic pathways is a well-known hallmark of cancer [154], as initially postulated by Judah Folkman in 1971 [155]. He proposed that tumor growth would stagnate at 1-2 mm^3 size without additional blood vessel recruitment. Therefore, targeting tumor vasculature would limit nutrient and oxygen supply to the tumor, thereby hindering growth and promoting regression [156]. Other authors alluded to restructuring tumor vasculature that would revert the disorganization and leakiness into a "normalized" phenotype [157]. As a positive side-effect to this mechanism of action, it was postulated that a normalization of the vasculature would lead to a more efficient cytotoxic drug delivery to the tumor and a decrease in the intratumoral fluid pressure [158].

Since these hypotheses were presented, and especially in the last two decades, targeting angiogenic pathways has gained much interest and resulted in effective anti-cancer treatment

strategies. These strategies include tyrosine kinase inhibitors (TKIs), which inhibit VEGF effects on effector cells, and monoclonal antibodies, which bind to and inhibit VEGF directly. While these agents have been found to be effective in a range of cancers (e.g., Kidney, lung, brain, colon), the contexts of use for these agents and optimal therapeutic combinations continue to be under investigation. A few studies have recently leveraged microfluidic models to study TKI effectiveness *in vitro* [55], including both in MVA models [40,62] and 3D scaffolding models[79]. Recent models have focused on renal cell carcinoma and, notably, evaluating personalized model responses to TKI agents [46,47]. Although these models are in their infancy, their use could be instrumental in determining the therapeutic effectiveness of combination therapies and optimizing therapeutic regimens.

Emerging topics and perspectives

The increased utilization of microfluidic technologies has led to great strides in angiogenesis research. These features have helped researchers better replicate *in vivo* environments while maintaining the experimental flexibility and analytical capability of *in vitro* models and independently evaluating factors driving angiogenesis. Recently, researchers in the field have increasingly included more physiologically relevant cues for the model at hand. These include patient-derived or iPSC cell sources, native extracellular matrices, and human serum [159]. Yet, the importance of each of these factors on angiogenesis remains to be elucidated on a model-to-model basis, such as the precise effects of shear stress in angiogenesis.

Novel and exciting angiogenesis models are recently emerging, such as lymphangiogenesis [81,82], retinal angiogenesis, and reproductive organ models [99,160]. The field is recognizing the great potential of microfluidic models in recapitulating these environments for basic biology or translational purposes. We anticipate that these and other applications will continue to emerge and gain interest in the field, leading to exciting research advances.

While the advances in microfluidic-enabled research are promising, widespread adoption of microfluidics remains a challenge. Specialized knowledge and training remain a necessity for aspiring microfluidic researchers. In response to this limitation, a great effort in the commercialization of microfluidic devices is underway, with dozens of companies filling the market need for easy-to-use microfluidic devices for *in vitro* modeling[27]. Furthermore, with a handful of PDMS-built models being validated through multiple different applications, it is reasonable for companies to invest in a transition to more large-scale fabrication methods capable of replacing the use of PDMS with more inert plastic-based alternatives. [11] Some other technical challenges that remain are the degree of control over the geometry, diameter, and layers of the vessels recapitulated, and the limited throughput of devices. Regarding the lack of control over vessel size, smaller vessels are currently recapitulated using MVA methods, which provide very limited control over the resulting network. Conversely, mold casting strategies typically produce larger vessels. However, none of these strategies are currently able to finely control the positioning of supporting cell types (e.g., pericytes)[29]. Bioprinting has been proposed as a potential solution to some of these challenges, as its resolution may increase to provide that additional layer of control over model building[161]. Finally, model tissue (also called organ-on-a-chip) vascularization remains an unresolved issue of interest for many biological fields.

Going forward, the advantages of microfluidic devices for recapitulating tissue pathophysiology by integrating spatial, biochemical, and biomechanical cues will likely provide insight into the mechanisms of angiogenesis, both in health and vascular-impacting diseases. Several research areas may benefit, especially from microfluidics, such as cardiac diseases[162] and regenerative therapy, where microfluidics can be used to study the disease pathology and generate new liquid biopsy diagnostic tools[163]. Likewise, there is an increasing interest in the field of neuroscience, where several microfluidic models of brain

microvasculature have been developed. Future microfluidic applications will likely investigate blood endothelial interactions, brain-blood barrier function, tissue vascularization, and the effect of angiogenic/anti-angiogenics drugs to treat conditions such as stroke or Alzheimer's. However, more work is needed to develop standardized devices that can be subject to clinical use approval.

The integration of relevant cues is also of importance in new drug discovery, where accurate cell behavior and response/resistance to therapies are fundamental. We anticipate that microfluidic models will serve as a complement to traditional *in vitro* testing. First the more accurate tissue mimicry may reveal new cell and tissue behaviors than those observed in traditional *in vitro* models. Further, microfluidic models are ideally suited to investigate therapeutic targets challenging to observe in traditional *in vitro* models, hence creating new research lines and therapeutic opportunities for vascular-related disorders.

Finally, we anticipate that the improved microenvironmental modeling of microfluidic systems will provide a more comprehensive risk-benefit assessment of newly developed therapies, both for drug development and from a precision medicine perspective. An example lies in TKI treatment of cancers. We anticipate TKI therapy will continue to be a relevant clinical treatment option. For example, combinations of TKI drugs [164] or TKI and immunotherapy agents (e.g., anti-PD-1/PD-L1) are getting FDA approval to treat several cancers, following evidence that TKIs play a role in overcoming resistance to immunotherapies. Thus, we foresee that microfluidic angiogenesis models will continue to complement traditional *in vitro* and *in vivo* models in assessing the effectiveness and safety of therapeutic combinations with TKI agents in individual patients.

Acknowledgments

Authors would like to acknowledge Dr Duane Juang for his comments on the fabrication section. This work was supported by the NIH (R33CA225281) and the Assistant Secretary of Defense for Health Affairs through the Prostate Cancer Research Program, Award No. W81XWH-18-1-0273 to DK. The U.S. Army Medical Research Acquisition Activity, 820 Chandler Street, Fort Detrick MD 21702-5014 is the awarding and administering acquisition office. Opinions, interpretations, conclusions and recommendations are those of the author and are not necessarily endorsed by the Department of Defense.

Author Contributions

Conceptualization: G.S., M.V., C.S., D.K.; Writing - Original Draft: G.S., M.V., C.S., Writing - Review & Editing: G.S., M.V., C.S., D.J.B., D.K.; Figure creation: M.V., C.S.; Supervision: D.K.; Funding acquisition: D.J.B., D.K.

Conflict of interest statement

David J. Beebe holds equity in Bellbrook Labs LLC, Tasso Inc., Salus Discovery LLC, Lynx Biosciences Inc., Stacks to the Future LLC, Turba LLC, Flambeau Diagnostics LLC, and Onexio Biosystems LLC. David J. Beebe is also a consultant for Abbott Laboratories.

References

1 P. Carmeliet and R. K. Jain, *Nature*, 2011, **473**, 298–307.
2 A. Fallah, A. Sadeghinia, H. Kahroba, A. Samadi, H. R. Heidari, B. Bradaran, S. Zeinali and O. Molavi, *Biomedicine & Pharmacotherapy*, 2019, **110**, 775–785.
3 G. Eelen, L. Treps, X. Li and P. Carmeliet, *Circulation Research*, 2020, **127**, 310–329.
4 D. Hanahan, *Perspectives on the Future of Angiogenesis Research*, Springer, Boston, MA, 2008.
5 M. Potente, H. Gerhardt and P. Carmeliet, *Cell*, 2011, **146**, 873–887.
6 S. Y. Yoo and S. M. Kwon, *Mediators of Inflammation*, 2012, **2013**
7 N. S. Vasudev and A. R. Reynolds, *Angiogenesis*, 2014, **17**, 471.
8 C. F. Buchanan, E. E. Voigt, C. S. Szot, J. Freeman, P. P. Vlachos and M. N. Rylander*, Tissue Engineering Part C: Methods*. 2013, **20**, 64–75.
9 B. M. Baker and C. S. Chen, *J Cell Sci*, 2012, **125**, 3015–3024.

10 A. Folch, *Introduction to bioMEMS*, CRC Press, 2016.
11 J. M. Ayuso, K.-Y. Park, M. Virumbrales-Muñoz and D. J. Beebe, *APL Bioengineering*, 2021, **5**, 010902.
12 E. Sollier, C. Murray, P. Maoddi, D. di Carlo, *Lab Chip*, 2011, **11**, 3752–3765.
13 D. B. Weibel, W. R. DiLuzio and G. M. Whitesides, *Nature Reviews Microbiology* 2007, **5**, 209–218.
14 D. I. Walsh, D. S. Kong, S. K. Murthy and P. A. Carr, *Trends in Biotechnology*, 2017, **35**, 383–392.
15 E. Berthier, E. W. K. Young and D. Beebe, *Lab on a Chip*, 2012, **12**, 1224–1237.
16 K. J. Regehr, M. Domenech, J. T. Koepsel, K. C. Carver, S. J. Ellison-Zelski, W. L. Murphy, L. A. Schuler, E. T. Alarid and D. J. Beebe, *Lab on a Chip*, 2009, **9**, 2132–2139.
17 A. Gokaltun, M. L. Yarmush, A. Asatekin and O. B. Usta, *Technology,* 2017, **05**, 1–12.
18 D. J. Guckenberger, T. E. de Groot, A. M. D. Wan, D. J. Beebe and E. W. K. Young, *Lab Chip*, 2015, **15**, 2364.
19 M. A. Câmara, J. C. C. Rubio, A. M. Abrão and J. P. Davim, *Journal of Materials Science & Technology*, 2012, **28**, 673–685.
20 M. Wilson, N. Kota, Y. Kim, Y. Wang, B. Stolz, P. LeDuc and O. Ozdoganlar, *Lab Chip*, 2011, **11**, 1550–1555.
21 E. Berthier, D. J. Guckenberger, P. Cavnar, A. Huttenlocher, N. Keller and D. J. Beebe, *Lab Chip*, 2013, **13**, 424–431.
22 Y. Ando, H. P. Ta, D. P. Yen, S.-S. Lee, S. Raola and K. Shen, *Scientific Reports*, 2017, **7**, 1–12.
23 I. Papautsky and E. T. K. Peterson, *Encyclopedia of Microfluidics and Nanofluidics*, 2015, 2102–2116.
24 R. Novak, N. Ranu and R. A. Mathies, *Lab Chip*, 2013, **13**, 1468.
25 S. J. Kim, H. Yang, K. Kim, Y. T. Lim and H. B. Pyo, *Electrophoresis*, 2006, **27**, 3284–3296.
26 G. Tosello, G. Bissacco, P. T. Tang, H. N. Hansen and P. C. Nielsen, *Microsystem Technologies*, 2008, **14**, 1757–1764.
27 B. Zhang and M. Radisic, *Lab Chip*, 2017, **17**, 2395–2420.
28 G. P. Raeber, M. P. Lutolf and J. A. Hubbell, *Biophysical Journal*, 2005, **89**, 1374–1388.
29 M. Virumbrales-Muñoz, J. M. Ayuso, M. M. Gong, M. Humayun, M. K. Livingston, K. M. Lugo-Cintrón, P. McMinn, Y. R. Álvarez-García and D. J. Beebe, *Chemical Society Reviews*, 2020, **49**, 6402–6442.
30 C. Tung, O. Krupa, E. Apaydin, J.-J. Liou, A. Diaz-Santana, B. J. Kim and M. Wu, *Lab on a Chip*, 2013, **13**, 3876–3885.
31 J. de Jong, R. G. H. Lammertink and M. Wessling, *Lab Chip*, 2006, **6**, 1125–1139.
32 I. Raimondi, L. Izzo, M. Tunesi, M. Comar, D. Albani and C. Giordano, *Frontiers in Bioengineering and Biotechnology*, , DOI:10.3389/fbioe.2019.00435.
33 Y. Choi, E. Hyun, J. Seo, C. Blundell, H. C. Kim, E. Lee, S. H. Lee, A. Moon, W. K. Moon and D. Huh, *Lab Chip*, 2015, **15**, 3350–3357.
34 G. Biffi and D. A. Tuveson, *Physiol Rev*, 2021, **101**, 147–176.
35 E. Sahai, I. Astsaturov, E. Cukierman, D. G. DeNardo, M. Egeblad, R. M. Evans, D. Fearon, F. R. Greten, S. R. Hingorani, T. Hunter, R. O. Hynes, R. K. Jain, T. Janowitz, C. Jorgensen, A. C. Kimmelman, M. G. Kolonin, R. G. Maki, R. S. Powers, E. Puré, D. C. Ramirez, R. Scherz-Shouval, M. H. Sherman, S. Stewart, T. D. Tlsty, D. A.

Tuveson, F. M. Watt, V. Weaver, A. T. Weeraratna and Z. Werb, *Nature Reviews Cancer* , 2020, **20**, 174–186.

36 D. Öhlund, A. Handly-Santana, G. Biffi, E. Elyada, A. S. Almeida, M. Ponz-Sarvise, V. Corbo, T. E. Oni, S. A. Hearn, E. J. Lee, I. I. C. Chio, C. il Hwang, H. Tiriac, L. A. Baker, D. D. Engle, C. Feig, A. Kultti, M. Egeblad, D. T. Fearon, J. M. Crawford, H. Clevers, Y. Park and D. A. Tuveson, *J Exp Med*, 2017, **214**, 579–596.

37 H. W. Kim, J. Lim, J. W. Rhie and D. S. Kim, *Microelectronic Engineering*, 2017, **174**, 24–27.

38 S. Pradhan, A. M. Smith, C. J. Garson, I. Hassani, W. J. Seeto, K. Pant, R. D. Arnold, B. Prabhakarpandian and E. A. Lipke, *Scientific Reports*, 2018, **8**, 1–15.

39 X. Wang, D. T. T. Phan, A. Sobrino, S. C. George, C. C. W. Hughes and A. P. Lee, *Lab Chip*, 2016, **16**, 282–290.

40 A. Sobrino, D. T. T. Phan, R. Datta, X. Wang, S. J. Hachey, M. Romero-López, E. Gratton, A. P. Lee, S. C. George and C. C. W. Hughes, *Scientific Reports* , 2016, **6**, 1–11.

41 D. T. T. Phan, X. Wang, B. M. Craver, A. Sobrino, D. Zhao, J. C. Chen, L. Y. N. Lee, S. C. George, A. P. Lee and C. C. W. Hughes, *Lab Chip*, 2017, **17**, 511–520.

42 V. S. Shirure, A. Lezia, A. Tao, L. F. Alonzo and S. C. George, *Angiogenesis*, 2017, **20**, 493–504.

43 M. Campisi, Y. Shin, T. Osaki, C. Hajal, V. Chiono and R. D. Kamm, *Biomaterials*, 2018, **180**, 117–129.

44 D. P. Lobo, A. M. Wemyss, D. J. Smith, A. Straube, K. B. Betteridge, A. H. J. Salmon, R. R. Foster, H. E. Elhegni, S. C. Satchell, H. A. Little, R. Pacheco-Gómez, M. J. Simmons, M. R. Hicks, D. O. Bates, A. Rodger, T. R. Dafforn and K. P. Arkill, *Nano Res*, 2015, **8**, 3307.

45 L. T. H. Dang, T. Aburatani, G. A. Marsh, B. G. Johnson, S. Alimperti, C. J. Yoon, A. Huang, S. Szak, N. Nakagawa, I. Gomez, S. Ren, S. K. Read, C. Sparages, A. C. Aplin, R. F. Nicosia, C. Chen, G. Ligresti and J. S. Duffield, *Biomaterials*, 2017, **141**, 314–329.

46 J. A. Jiménez-Torres, M. Virumbrales-Muñoz, K. E. Sung, M. H. Lee, E. J. Abel and D. J. Beebe, *EBioMedicine*, 2019, **42**, 408–419.

47 María Virumbrales-Muñoz, Jiong Chen, Jose Ayuso, Moonhee Lee, E. Jason Abel and D. J. Beebe, *Lab Chip*, 2020, **20**, 4420–4432.

48 D. (Dan) Huh, *Ann Am Thorac Soc*, 2015, **12**, S42–S44.

49 B. A. Hassell, G. Goyal, E. Lee, A. Sontheimer-Phelps, O. Levy, C. S. Chen and D. E. Ingber, *Cell Rep*, 2017, **21**, 508–516.

50 P. A. Galie, D.-H. T. Nguyen, C. K. Choi, D. M. Cohen, P. A. Janmey and C. S. Chen, *Proceedings of the National Academy of Sciences*, 2014, **111**, 7968–7973.

51 I. K. Zervantonakis, S. K. Hughes-Alford, J. L. Charest, J. S. Condeelis, F. B. Gertler and R. D. Kamm, *Proceedings of the National Academy of Sciences*, 2012, **109**, 13515–13520.

52 B. Kwak, A. Ozcelikkale, C. S. Shin, K. Park and B. Han, *Journal of Controlled Release*, 2014, **194**, 157–167.

53 K. Hockemeyer, C. Janetopoulos, A. Terekhov, W. Hofmeister, A. Vilgelm, L. Costa, J. Wikswo and A. Richmond, *Biomicrofluidics,* 2018, **12**, 034102.

54 M. Virumbrales-Muñoz, J. M. Ayuso, M. Olave, R. Monge, D. de Miguel, L. Martínez-Lostao, S. le Gac, M. Doblare, I. Ochoa and L. J. Fernandez, *Scientific Reports*, 2017, **7**, 1–15.

55 C. P. Miller, C. Tsuchida, Y. Zheng, J. Himmelfarb, S. Akilesh, M. CP, T. C, Z. Y, H. J and A. S, *Neoplasia*, 2018, **20**, 610–620.

56 G. S. Offeddu, L. Possenti, J. T. Loessberg-Zahl, P. Zunino, J. Roberts, X. Han, D. Hickman, C. G. Knutson and R. D. Kamm, *Small*, 2019, **15**, 1902393.

57 K. Haase, M. R. Gillrie, C. Hajal and R. D. Kamm, *Advanced Science*, 2019, **6**, 1900878.

58 J. S. Jeon, S. Bersini, J. A. Whisler, M. B. Chen, G. Dubini, J. L. Charest, M. Moretti and R. D. Kamm, *Integrative Biology*, 2014, **6**, 555–563.

59 K. A. DiVito, M. A. Daniele, S. A. Roberts, F. S. Ligler and A. A. Adams, *Data in Brief*, 2017, **14**, 156–162.

60 Y. Nashimoto, T. Hayashi, I. Kunita, A. Nakamasu, J. Torisawa, M. Nakayama, H. Takigawa-Imamura, H. Kotera, K. Nishiyama, T. Miura and R. Yokokawa, *Integr Biol (Camb)*, 2017, **9**, 506–518.

61 M. Gilardi, S. Bersini, S. Valtorta, M. Proietto, M. Crippa, A. Boussommier-Calleja, M. Labelle, R. M. Moresco, M. Vanoni, R. D. Kamm and M. Moretti, *Biomaterials*, 2021, **276**, 120975.

62 S. Zeinali, C. A. Bichsel, N. Hobi, M. Funke, T. M. Marti, R. A. Schmid, O. T. Guenat and T. Geiser, *Angiogenesis*, 2018, **21**, 861–871.

63 X. Zhang, D. Huk, Q. Wang, J. Lincoln, Y. Zhao, X. Zhang, D. J. Huk, Q. Wang, J. Lincoln and Y. Zhao, *Biomicrofluidics*, 2014, **8**, 054106.

64 E. Westein, A. D. van der Meer, M. J. E. Kuijpers, J.-P. Frimat, A. van den Berg and J. W. M. Heemskerk, *Proceedings of the National Academy of Sciences*, 2013, **110**, 1357–1362.

65 T. S. Frost, L. Jiang, R. M. Lynch and Y. Zohar, *Micromachines (Basel)*, 2019, **10**, 533.

66 D. Huh, B. D. Matthews, A. Mammoto, M. Montoya-Zavala, Y. H. Hsin and D. E. Ingber, *Science*, 2010, **328**, 1662–1668.

67 J. W. Song, D. Bazou and L. L. Munn, *Methods in Molecular Biology*, 2015, **1214**, 243–254.

68 J. W. Song and L. L. Munn, *Proceedings of the National Academy of Sciences*, 2011, **108**, 15342–15347.

69 M. Carden, M. Fay, X. Lu, R. G. Mannino, Y. Sakurai, J. C. Ciciliano, C. E. Hansen, S. Chonat, J. CH, W. DK and L. WA, *Blood*, 2017, **130**, 2654–2663.

70 V. Introini, A. Carciati, G. Tomaiuolo, P. Cicuta and S. Guido, *Journal of the Royal Society Interface*, 2018, **15**, 20180773.

71 H. Y. Chen, H. der Tsai, W. C. Chen, J. Y. Wu, F. J. Tsai and C. H. Tsai, *Journal of Clinical Laboratory Analysis*, 2001, **15**, 251–255.

72 D. Tsvirkun, A. Grichine, A. Duperray, C. Misbah and L. Bureau, *Scientific Reports*, 2017, **7**, 1–11.

73 G. S. Jeong, S. Han, Y. Shin, G. H. Kwon, R. D. Kamm, S.-H. Lee and S. Chung, *Analytical Chemistry*, 2011, **83**, 8454–8459.

74 C. del Amo, C. Borau, R. Gutiérrez, J. Asín and J. M. García-Aznar, *J Biomech*, 2016, **49**, 1340–1346.

75 S. Kim, M. Chung, J. Ahn, S. Lee and N. L. Jeon, *Lab Chip*, 2016, **16**, 4189–4199.

76 M. Campisi, S. Sundararaman, S. E. Shelton, E. H. Knelson, N. R. Mahadevan, R. Yoshida, T. Tani, E. Ivanova, I. Cañadas, T. Osaki, S. W. L. Lee, T. Thai, S. Han, B. P. Piel, S. Gilhooley, C. P. Paweletz, V. Chiono, R. D. Kamm, S. Kitajima and D. A. Barbie, *Front Immunol*, 2020, **11**, 2090.

77 K. Haase, G. S. Offeddu, M. R. Gillrie and R. D. Kamm, *Adv Funct Mater*, 2020, **30**, 2002444.

78 V. van Duinen, D. Zhu, C. Ramakers, A. J. van Zonneveld, P. Vulto and T. Hankemeier, *Angiogenesis*, 2019, **22**, 157–165.

79 S. Lee, S. Kim, D.-J. Koo, J. Yu, H. Cho, H. Lee, J. M. Song, S.-Y. Kim, D.-H. Min and N. L. Jeon, *ACS Nano*, 2020, **15**, 338–350.

80 C. F. Buchanan, S. S. Verbridge, P. P. Vlachos and M. N. Rylander, *Cell Adh Migr*, 2015, **8**, 517–524.

81 K. M. Lugo-Cintrón, J. M. Ayuso, B. R. White, P. M. Harari, S. M. Ponik, D. J. Beebe, M. M. Gong and M. Virumbrales-Muñoz, *Lab Chip*, 2020, **20**, 1586–1600.

82 K. M. Lugo-Cintrón, J. M. Ayuso, M. Humayun, M. M. Gong, S. C. Kerr, S. M. Ponik, P. M. Harari, M. Virumbrales-Muñoz and D. J. Beebe, *EBioMedicine*, 2021, **73**, 103634.

83 L. L. Bischel, S.-H. Lee and D. J. Beebe, *J Lab Autom*, 2012, **17**, 96–103.

84 K. M. Lugo-Cintrón, M. M. Gong, J. M. Ayuso, L. Tomko, D. J. Beebe, M. Virumbrales-Muñoz and S. M. Ponik, *Cancers (Basel)*, 2020, **12**, 1173.

85 D.-H. T. Nguyen, S. C. Stapleton, M. T. Yang, S. S. Cha, C. K. Choi, P. A. Galie and C. S. Chen, *Proceedings of the National Academy of Sciences*, 2013, **110**, 6712–6717.

86 J. A. Jiménez-Torres, S. L. Peery, K. E. Sung and D. J. Beebe, *Advanced Healthcare Materials*, 2016, **5**, 198–204.

87 L. L. Bischel, S.-H. Lee and D. J. Beebe, *Journal of Laboratory Automation,* 2012, **17**, 96–103.

88 J. Yu, E. Berthier, A. Craig, T. de Groot, S. Sparks, P. Ingram, D. Jarrard, W. Huang, D. J. Beebe and A. Theberge, *Nat Biomed Eng*, 2019, **3**, 830–841.

89 L. L. Bischel, K. E. Sung, J. A. Jiménez-Torres, B. Mader, P. J. Keely and D. J. Beebe, *The FASEB Journal*, 2014, **28**, 4583–4590.

90 S. J. Trietsch, E. Naumovska, D. Kurek, M. Setyawati, M. K. Vormann, K. J. Wilschut, H. L. Lanz, A. Nicolas, C. P. Ng, J. Joore, S. Kustermann, A. Roth, T. Hankemeier, A. Moisan and P. Vulto, *Nat Commun*, 2017, **8**, 1–8.

91 M. M. Morgan, M. K. Livingston, J. W. Warrick, E. M. Stanek, E. T. Alarid, D. J. Beebe and B. P. Johnson, *Molecules*, 2018, **8**, 1–13.

92 T. J. Poole and J. D. Coffin, *J Exp Zool*, 1989, **251**, 224–231.

93 W. Risau, *Nature*, 1997, **386**, 671–674.

94 I. Flamme, T. Frölich and W. Risau, *J Cell Physiol*, 1997, **173**, 206–10.

95 S. Kim, H. Lee, M. Chung and N. L. Jeon, *Lab Chip*, 2013, **13**, 1489–1500.

96 J. J. H. Kim, M. Chung, S. Kim, D. H. Jo, J. J. H. Kim and N. L. Jeon, *PLOS ONE*, 2015, **10**, e0133880.

97 J. M. Ayuso, M. Virumbrales-Muñoz, J. M. Lang and D. J. Beebe, *Nature Communications*, 2022, **13**, 3086.

98 W. J. Polacheck, M. L. Kutys, J. Yang, J. Eyckmans, Y. Wu, H. Vasavada, K. K. Hirschi and C. S. Chen, *Nature*, 2017, **552**, 258–262.

99 Y. Qiu, B. Ahn, Y. Sakurai, C. E. Hansen, R. Tran, P. N. Mimche, R. G. Mannino, J. C. Ciciliano, T. J. Lamb, C. H. Joiner, S. F. Ofori-Acquah and W. A. Lam, *Nature Biomedical Engineering*, 2018, **2**, 453–463.

100 K. Funamoto, I. K. Zervantonakis, Y. Liu, C. J. Ochs, C. Kim and R. D. Kamm, *Lab Chip*, 2012, **12**, 4855–4863.

101 N. Jusoh, J. Ko and N. L. Jeon, *APL Bioengineering*, 2019, **3**, 36101.

102 David J. Beebe, and Glennys A. Mensing and G. M. Walker, *Annu Rev Biomed Eng*, 2003, **4**, 261–286.
103 B. J. Ballermann, A. Dardik, E. Eng and A. Liu, *Kidney International*, 1998, **54**, S100–S108.
104 S. Chatterjee, *Frontiers in Physiology*, 2018, **0**, 524.
105 K. S. Cunningham and A. I. Gotlieb, *Lab Invest*, 2005, **85**, 9–23.
106 J. Scallan, V. H. Huxley and R. J. Korthuis, *Fluid Movement Across the Endothelial Barrier*, Morgan & Claypool Life Sciences, 2010.
107 A. Siddique, T. Meckel, R. W. Stark and S. Narayan, *Colloids and Surfaces B: Biointerfaces*, 2017, **150**, 456–464.
108 J. W. Song, D. Bazou and L. L. Munn, *Methods in Molecular Biology*, 2015, **1214**, 243–254.
109 C. F. Buchanan, E. E. Voigt, C. S. Szot, J. W. Freeman, P. P. Vlachos and M. N. Rylander, *Tissue Engineering Part C: methods*, 2014, **20**, 64–75.
110 S. H. Wu, F. Zhang, S. Yao, L. Tang, H. T. Zeng, L. P. Zhu and Z. Yang, *International Journal of Stem Cells*, 2020, **13**, 312-325.
111 C. A. Hesh, Y. Qiu and W. A. Lam, *Micromachines (Basel)*, 2019, **1**, 18.
112 J. White, S. Krishnamoorthy, D. Gupta, M. Lancelot, N. Moore, S. Sarnaik, W. E. Hobbs, D. R. Light and P. Hines, *British Journal of Haematology*, 2016, **174**, 970–982.
113 M. Tsai, A. Kita, J. Leach, R. Rounsevell, J. N. Huang, J. Moake, R. E. Ware, D. A. Fletcher and W. A. Lam, *The Journal of Clinical Investigation*, 2012, **122**, 408–418.
114 R. Barrile, A. van der Meer, H. Park, J. Fraser, D. Simic, F. Teng, D. Conegliano, J. Nguyen, A. Jain, M. Zhou, J. Karalis, D. E. Ingber, G. Hamilton and M. Otieno, *Clin Pharmacol Ther*, 2018, **104**, 1240–1248.
115 X. Wu, M. Newbold, Z. Gao and C. Haynes, *Biochim Biophys Acta Gen Subj*, 2017, **1861**, 1122–1130.
116 B. Yue, *J Glaucoma*, 2014, **23**, S20.
117 M. Mongiat, E. Andreuzzi, G. Tarticchio and A. Paulitti, *International Journal of Molecular Sciences*, 2016, **17**, 1822.
118 W. J. Polacheck and C. S. Zhang, *Nat Methods*, 2016, **13**, 415–423.
119 S. Syed, A. Karadaghy and S. Zustiak, *Journal of Visualized Experiments : JoVE*, 2015, **2015**, 52643.
120 H. H. See, S. C. B. Herath, R. Arayanarakool, Y. Du, E. Tan, R. Ge, H. Asadam and P. C. Y. Chen, *SLAS Technol*, 2018, **23**, 70–82.
121 J. Keys, A. Windsor and J. Lammerding, *Methods Mol Biol*, 2018, **1840**, 101–118.
122 K. M. Chrobak, D. R. Potter and J. Tien, *Microvasc Res*, 2006, **71**, 185–196.
123 V. Silvestri, E. Henriet, R. Linville, A. Wong, P. Searson and A. Ewald, *Cancer Res*, 2020, **80**, 4288–4301.
124 C. M. Ghajar, X. Chen, J. W. Harris, V. Suresh, C. C. W. Hughes, N. L. Jeon, A. J. Putnam and S. C. George, *Biophysical Journal*, 2008, **94**, 1930–1941.
125 M. M. Martino, S. Brkic, E. Bovo, M. Burger, D. J. Schaefer, T. Wolff, L. Gürke, P. S. Briquez, H. M. Larsson, R. Gianni-Barrera, J. A. Hubbell and A. Banfi, *Frontiers in Bioengineering and Biotechnology*, 2015, **0**, 45.
126 S. Sokic and G. Papavasiliou, *Tissue Engineering Part A*, 2012, **18**, 2477–2486.
127 W. Y. Wang, R. N. Kent, S. A. Huang, E. H. Jarman, E. H. Shikanov, C. D. Davidson, H. L. Hiraki, D. Lin, M. A. Wall, D. L. Matera, J.-W. Shin, W. J. Polacheck, A. Shikanov and B. M. Baker, *Acta Biomaterialia*, 2021, **135**, 260–273.

128 B. Trappmann, B. M. Baker, W. J. Polacheck, C. K. Choi, J. A. Burdick and C. S. Chen, *Nature Communications 2017 8:1*, 2017, **8**, 1–8.

129 B. M. Baker, B. Trappmann, S. C. Stapleton, E. Toro and C. S. Chen, *Lab Chip*, 2013, **13**, 3246–3252.

130 A. Neve, F. P. Cantatore, N. Maruotti, A. Corrado and D. Ribatti, *BioMed Research International*, 2014, **2014**.

131 A. H. Sprague and R. A. Khalil, *Biochem Pharmacol*, 2009, **78**, 539.

132 Y. Shin, J. S. Jeon, S. Han, G.-S. Jung, S. Shin, S.-H. Lee, R. Sudo, R. D. Kamm and S. Chung, *Lab Chip*, 2011, **11**, 2175–2181.

133 H. M. Swartz and J. F. Dunn, *Advances in Experimental Medicine and Biology*, 2003, **530**, 1–12.

134 V. S. Shirure, S. F. Lam, B. Shergill, Y. E. Chu, N. R. Ng and S. C. George, *Lab on a Chip*, 2020, **20**, 3036–3050.

135 K. R. Rivera, M. A. Yokus, P. D. Erb, V. A. Pozdin and M. Daniele, *Analyst*, 2019, **144**, 3190–3215.

136 J. M. Ayuso, R. Monge, G. A. Llamazares, M. Moreno, M. Agirregabiria, J. Berganzo, M. Doblaré, I. Ochoa and L. J. Fernández, *Frontiers in Materials*, 2015, **0**, 37.

137 D. A. Markov, E. M. Lillie, S. P. Garbett and L. J. McCawley, *Biomedical Microdevices 2013 16:1*, 2013, **16**, 91–96.

138 S. F. Lam, V. S. Shirure, Y. E. Chu, A. G. Soetikno and S. C. George, *PLOS ONE*, 2018, **13**, e0209574.

139 H.-H. Hsu, P.-L. Ko, H.-M. Wu, H.-C. Lin, C.-K. Wang and Y.-C. Tung, *Small*, 2021, **17**, 2006091.

140 M. Virumbrales-Muñoz, J. M. Ayuso, J. R. Loken, K. M. Denecke, S. Rehman, M. C. Skala, E. J. Abel and D. J. Beebe, *Biomaterials*, 2022, **283**, 121454.

141 M. M. Morgan, B. P. Johnson, M. K. Livingston, L. A. Schuler, E. T. Alarid, K. E. Sung and D. J. Beebe, *Pharmacology & Therapeutics*, 2016, **165**, 79–92.

142 S. F. Rodrigues and D. N. Granger, *Tissue Barriers*, 2015, **3,** e978720.

143 F. R. Walter, S. Valkai, A. Kincses, A. Petneházi, T. Czeller, S. Veszelka, P. Ormos, M. A. Deli and A. Dér, *Sensors and Actuators B: Chemical*, 2016, **222**, 1209–1219.

144 K. Sellgren, B. Hawkins and S. Grego, *Biomicrofluidics*, 2015, **9**, 061102.

145 T. B. Terrell-Hall, A. G. Ammer, J. I. G. Griffith and P. R. Lockman, *Fluids and Barriers of the CNS*, 2017, **14**, 3.

146 V. Martínez-Redondo, A. T. Pettersson and J. L. Ruas, *Diabetologia*, 2015, **58**, 1969–1977.

147 J. A. Brown, V. Pensabene, D. A. Markov, V. Allwardt, M. D. Neely, M. Shi, C. M. Britt, O. S. Hoilett, Q. Yang, B. M. Brewer, P. C. Samson, L. J. McCawley, J. M. May, D. J. Webb, D. L. Li, A. B. Bowman, R. S. Reiserer and J. P. Wikswo, *Biomicrofluidics*, 2015, **9**, 054124.

148 R. Augustine, A. H. Aqel, S. N. Kalva, K. S. Joshy, A. Nayeem and A. Hasan, *Translational Oncology*, 2021, **14**, 101087.

149 J. A. Kim, H. N. Kim, S.-K. Im, S. Chung, J. Y. Kang and N. Choi, *Biomicrofluidics*, 2015, **9**, 024115.

150 E. A. Runkle and D. A. Antonetti, *Methods Mol Biol*, 2011, **686**, 133–148.

151 Y. B. Arık, W. Buijsman, J. Loessberg-Zahl, C. Cuartas-Vélez, C. Veenstra, S. Logtenberg, A. M. Grobbink, P. Bergveld, G. Gagliardi, A. I. den Hollander, N. Bosschaart, A. van den Berg, R. Passier and A. D. van der Meer, *Lab Chip*, 2021, **21**, 272–283.

152 J. M. Chan, I. K. Zervantonakis, T. Rimchala, W. J. Polacheck, J. Whisler and R. D. Kamm, *PLOS ONE*, 2012, **7**, e50582.
153 S. Chen, L. Zhang, Y. Zhao, M. Ke, B. Li, L. Chen and S. Cai, *Biomicrofluidics*, 2017, **11**, 054111.
154 D. Hanahan and R. A. Weinberg, *Cell*, 2000, **100**, 57–70.
155 J. Folkman, *The New England Journal of Medicine*, 2010, **285**, 1182–1186.
156 Y. He, M. Halford, M. Achen and SA. Stacker, *Biochem Soc Trans*, 2014, **42**, 1569–1575.
157 P. Carmeliet and R. K. Jain, *Nat Rev Drug Discov*, 2011, **10**, 417–427.
158 R. K. Jain, *Nature Medicine*, 2001, **7**, 987–989.
159 D. B. Chou, V. Frismantas, Y. Milton, R. David, P. Pop-Damkov, D. Ferguson, A. MacDonald, Ö. Vargel Bölükbaşı, C. E. Joyce, L. S. Moreira Teixeira, A. Rech, A. Jiang, E. Calamari, S. Jalili-Firoozinezhad, B. A. Furlong, L. R. O'Sullivan, C. F. Ng, Y. Choe, S. Marquez, K. C. Myers, O. K. Weinberg, R. P. Hasserjian, R. Novak, O. Levy, R. Prantil-Baun, C. D. Novina, A. Shimamura, L. Ewart and D. E. Ingber, *Nature Biomedical Engineering* , 2020, **4**, 394–406.
160 E. S. Gargus, H. B. Rogers, K. E. McKinnon, M. E. Edmonds and T. K. Woodruff, *Nature Biomedical Engineering*, 2020, **4**, 381–393.
161 E. P. Chen, Z. Toksoy, B. A. Davis and J. P. Geibel, *Frontiers in Bioengineering and Biotechnology*, 2021, **9**, 664188
162 Q. Ma, H. Ma, F. Xu, X. Wang and W. Sun, *Microsystems & Nanoengineering* , 2021, **7**, 1–19.
163 A. Bluecher, S. M. dos Santos, N. Ferreirós, S. Labocha, I. M. R. Meyer Dos Santos, B. Picard-Willems, S. Harder and O. C. Singer, *Thromb Haemost*, 2017, **117**, 519–528.
164 V. M. Garcia, B. Basu, L. R. Molife and S. B. Kaye, *Clinical Cancer Research*, 2012, **18**, 3750–3761.